Catalysis Science & Technology

COMMUNICATION

View Article Online
View Journal | View Issue

Cite this: Catal. Sci. Technol., 2016, 6, 404

Received 4th September 2015,
Accepted 2nd October 2015

DOI: 10.1039/c5cy01476j

www.rsc.org/catalysis

Hydrogenation of CO_2 to formic acid with iridium^{III}(bisMETAMORPhos)(hydride): the role of a dormant *fac*-Ir^{III}(trihydride) and an active *trans*-Ir^{III}(dihydride) species†

S. Oldenhof, J. I. van der Vlugt* and J. N. H. Reek*

An Ir^{III}-monohydride species bearing a chemoresponsive ligand is active in catalytic CO_2 hydrogenation to formic acid with DBU as the exogenous base. Spectroscopic and computational data reveal a *trans*-Ir^{III}-dihydride as the essential catalytic intermediate and an Ir^{III}(H)$_3$ species as the dormant off-cycle product. This insight will aid future design of improved CO_2 reduction catalysts.

Carbon dioxide utilization has attracted much interest in academia and industry. This relates to renewable energy applications and as an alternative C_1 carbon building block in synthesis.[1] In particular, its reduction to formic acid (HCOOH) has been investigated intensively, given its potential as a reversible hydrogen storage system, alongside other commercial applications in *e.g.* the rubber, agricultural and textile industries.[2] The hydrogenation of CO_2 to HCOOH is endergonic by 33 kJ mol^{-1} mainly because of a large loss in entropy (eqn (1)). Temperature, pressure, solvent and additives can be used to influence the equilibrium of this reaction. CO_2 hydrogenation is often performed with addition of an external base such as ammonia or NEt_3, as this results in a thermodynamically more stable formate–base ion pair, which drives the equilibrium toward HCOOH formation (eqn (2)).

$$H_2(g) + CO_2(g) \rightleftharpoons HCOOH(l) \quad \Delta G^0 = 33\ \text{kJ mol}^{-1} \tag{1}$$

$$H_2(aq) + CO_2(aq) + NH_3(aq) \rightleftharpoons HCO_2^-(aq) + NH_4^+(aq) \quad \Delta G^0 = -35\ \text{kJ mol}^{-1} \tag{2}$$

The most active homogeneous catalysts to date for CO_2 hydrogenation to HCOOH under basic conditions are based on either Ir or Ru (Fig. 1; **A–C**).[3–5] Outer-sphere interactions such as hydrogen bonding and chemoresponsive ligand reactivity were found to play an essential role in these catalysts to ensure efficient turnover.[5–8] The importance of outer-sphere interactions has also been established for various systems specifically reported to catalyze the microscopic reverse process, *i.e.* formic acid dehydrogenation.[9,10] Similar outer-sphere interactions were reported for an iridium-trihydride complex **D-CO$_2$** bearing a chemoresponsive PNP ligand that engages in a stabilizing hydrogen bond interaction with CO_2.[11] DFT calculations have been used to postulate a correlation between the Ir–H$_{axial}$ bond length and the relative free energy ΔG^0 of CO_2 insertion: a longer Ir–H$_{axial}$ bond length (*i.e.* weaker bond) enhances Ir formate formation (*i.e.* facilitates CO_2 insertion). A related correlation between the hydricity of an Ir–H fragment and the rate of CO_2 insertion has recently been formulated, again based on a computational study.[12]

We previously reported the secondary interactions between formic acid and Ir^{III}(H)(bisMETAMORPhos) complex **1** to form **1-HCOOH** (Fig. 1) as being relevant for the dehydrogenation of HCOOH.[13] The reactive bis(sulfonamidophosphine) ligand in complex **1-HCOOH** functions both as an internal base to deprotonate HCOOH and as a hydrogen bond donor/acceptor to pre-assemble HCOOH and stabilize catalytically relevant transition states. Herein, we report initial data for catalytic CO_2 hydrogenation with Ir^{III}(H)(bisMETAMORPhos) complex **1** and discuss the role of a relatively unreactive *fac*-Ir^{III}(H)$_3$ species, which is formed under the applied reaction conditions, based on *in situ* NMR experiments and DFT calculations. This insight may aid future catalyst design for metal–ligand bifunctional CO_2 hydrogenation.

To monitor the catalytic activity of complex **1** in CO_2 hydrogenation, high-pressure NMR experiments were performed at 373 K and 50 bar of CO_2 and H_2 (1 : 1 ratio) in DMSO-d_6, using DMF (0.5 M) as the internal standard and in the absence of an external base.[14] Moderate catalytic activity for CO_2 hydrogenation was observed, with a turnover

Homogeneous, Bioinspired & Supramolecular Catalysis, van't Hoff Institute for Molecular Sciences, University of Amsterdam, Science Park 904, 1098 XH Amsterdam, The Netherlands. E-mail: j.i.vandervlugt@uva.nl, j.n.h.reek@uva.nl

† Electronic supplementary information (ESI) available: Experimental and computational details. See DOI: 10.1039/c5cy01476j

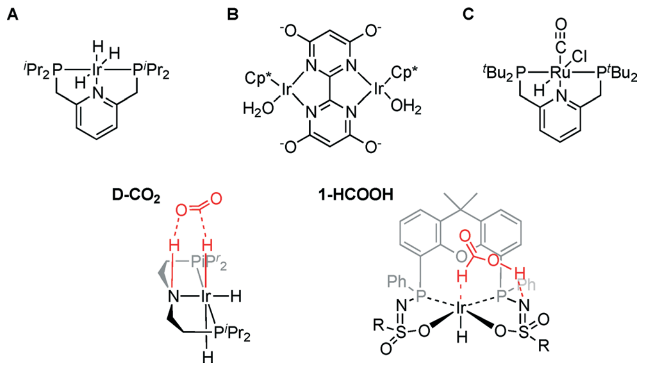

Fig. 1 Catalysts **A**–**C** and **D-CO$_2$** for CO_2 hydrogenation to HCOOH and the formic acid adduct of Ir^{III}(H)(bisMETAMORPhos) complex **1** (**1-HCOOH**; R = 4-butylbenzene).

frequency (TOF) of 18 h^{-1} in the first 30 minutes of the reaction and a turnover number (TON) of 30 after 90 minutes (Fig. 2, green curve). The conversion did not increase significantly between 90 and 180 minutes and a final concentration of 0.015 M HCOOH was obtained.

When catalysis was performed under the same catalytic conditions but in the presence of 1.0 mmol (0.5 M) of NEt_3, only a slight increase in activity was observed (Fig. 2, red curve). In contrast to this negligible effect of NEt_3 on the catalytic performance, the addition of 1.0 mmol of DBU (1,8-diazabicyclo[5.4.0]undec-7-ene) led to a significant improvement in the catalytic activity, with a TOF of 636 h^{-1} between 0–30 minutes and a TON of 685 after 180 minutes (Fig. 2, blue curve), corresponding to a base conversion of 0.685.‡ The remarkable effect of the base on the catalytic activity can be explained by the difference in basicity in DMSO (DBU: pK_a 12.0; NEt_3: pK_a 9.0). Similar differences in the catalytic performance of NEt_3 and DBU were observed in system **C**.[5] The

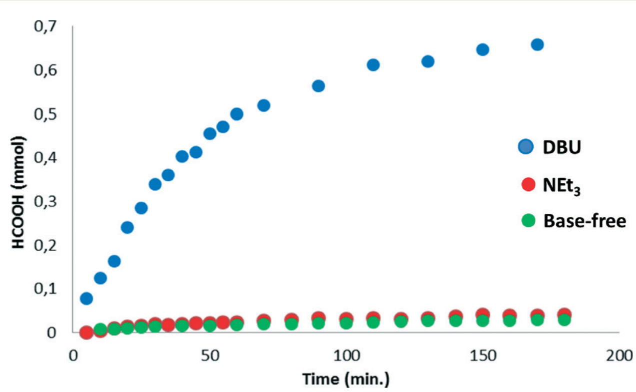

Fig. 2 Catalytic CO_2 hydrogenation with **1** (0.5 mM) under base-free conditions (green) and with the addition of 1000 equiv. (0.5 M) of NEt_3 (red) or DBU (blue). Solvent: DMSO-d_6, T = 373 K, total reaction volume = 2 mL. The absolute amount of HCOOH produced in mmol is plotted *vs.* time in minutes.

‡ Significant loss of catalytic activity is observed over time, likely due to a pressure drop in the NMR tube during turnover; see the ESI.†

formation of $HDBU^+ \cdot HCOO^-$ was monitored over time by the appearance of the $HCOO^-$ formate signal at 8.60 ppm in consecutive ^1H NMR spectra (see the ESI†). The concentration of H_2 increases over time, but is barely detectable in the first 30 minutes of reaction. The determined initial rates are therefore likely limited by mass transfer. Various solvents were used as reaction media but this did not lead to enhanced catalytic activities. In dioxane, a slight decrease in TOF was observed (588 h^{-1}), while in ethylene glycol, the catalytic activity decreased significantly (TOF: 38 h^{-1}). To obtain more insight into the mechanism of CO_2 hydrogenation, complex **1** was studied by ^1H NMR spectroscopy under combined H_2 and CO_2 pressure in the absence of a base. When **1** was dissolved in CD_2Cl_2, a well-defined triplet was observed in the ^1H NMR spectrum at δ −28.7 ppm (Fig. 3A) as previously reported.[13] However, when **1** was dissolved in DMSO-d_6, six different hydride signals were detected in the region from δ −24.0 to −29.0 ppm (Fig. 3B).

The generation of these species may result from: (1) the coordination of either DMSO, H_2O or the oxygen of the xanthene backbone to the vacant axial site of complex **1**,¶ (2) the dimer formation to give $\{(1)_2\}$ as previously observed in the solid state[13] or (3) the formation of different diastereomers by rotation of the sulfone group. Molecular structures of both a dimer and an axial H_2O adduct of complex **1** have been reported.[13] Upon pressurizing a DMSO-d_6 solution of **1** in a high-pressure sapphire NMR tube with 50 bar CO_2/H_2 (1 : 1)

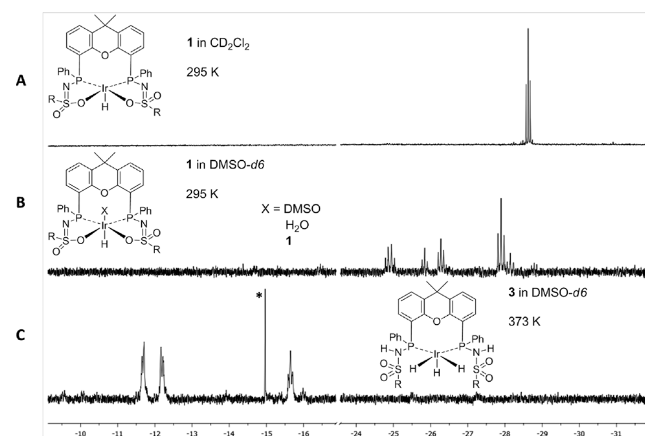

Fig. 3 ^1H NMR spectra of (A) **1** dissolved in CD_2Cl_2, (B) **1** dissolved in DMSO-d_6, and (C) formation of **3** from **1** with H_2/CO_2 (25/25 bar) at 373 K in DMSO-d_6, R = 4-butylbenzene. * indicates a minor impurity.§

§ The formation of **3** is accompanied by a species 'A' displaying a sharp singlet at −15.0 ppm (*). The ratio of **3** to 'A' remains unchanged over time. This complex is thus likely not a derivative of **1**, nor does it match previously described deactivation products.[18] Stirring Ir(acac)(cod) in DMSO-d_6 under 50 bar CO_2/H_2 (1 : 1) at 373 K resulted in identical spectral features (Ir(acac)(cod) is added in slight excess (5%) during the synthesis of **1**). This unidentified complex is a poor CO_2 hydrogenation catalyst (TON of 1.9 after 90 minutes at 373 K).

¶ DMSO is known to have several coordination modes: κ^1-*O*, κ^1-*S*, and κ^2-*S*,*O*. Species with the xanthene oxygen coordinated to Ir were all found to be close in energy based on DFT calculations [BP86, SV(P)].

at room temperature, no changes were observed in the ^{1}H NMR spectrum after one hour. Heating the sample to 373 K led to the formation of a new species that displayed two broad hydride signals: a doublet-of-doublets at δ −11.9 ppm ($^2J_{P-H}$ of 154.3 and 14.9 Hz) and a triplet at δ −15.7 ppm ($^2J_{P-H}$ of 17.7 Hz) in a 2:1 ratio (Fig. 3C). The coupling constants observed for the doublet-of-doublets are indicative of *trans* (154.3 Hz) and *cis* ^{31}P–^{1}H coupling (14.9 Hz), while the triplet originates from coupling of a hydride to two *cis*-positioned phosphorus nuclei. In the corresponding phosphorus-decoupled ^{1}H NMR spectrum, two singlets were observed. The ratio of the two hydride signals proved to be independent of temperature, suggesting that they belong to a single species. Together, this suggests the formation of five-coordinate trihydride complex **3**, *fac*-Ir^{III}(H)$_3$(bisMETAMORPhos) (see Scheme 1). Related *fac*-Ir^{III}(H)$_3$ complexes with Xantphos show similar spin systems.[15] The $^2J_{H-H}$ couplings, which are typically in the range of 2.6–7.4 Hz, could not be resolved due to broadening of the spectrum at 373 K. The N–H resonances of the protonated ligand arms could not be identified by ^{1}H NMR spectroscopy, as they tend to overlap with aromatic signals.[13,16] After releasing the CO_2/H_2 pressure, **3** remained stable for at least one hour at room temperature. Upon re-heating the depressurized solution to 373 K, the hydride signals corresponding to **3** disappeared and complex **1** was regenerated, concomitant with the formation of H_2, showing that the formation of **3** from **1** is reversible (Scheme 1).

Species **1** is stable under pure CO_2, but NMR signals that indicate the slow formation of **3** appear under pure H_2 atmosphere. The formation of **3** is suggested to proceed *via* the formation of intermediate **2** through heterolytic splitting of H_2 by **1**, as previously described.[13,16] Subsequently, another equivalent of H_2 is activated, presumably also in a heterolytic fashion, by decoordination of the neutral ligand arm to generate a vacant site and with the anionic ligand arm acting as an internal base, resulting in the square pyramidal *fac*-Ir^{III}(H)$_3$(bisMETAMORPhos) species **3**.

Interestingly, prior to the formation of **3**, the generation of 14 equivalents of HCOOH was evidenced by ^{1}H NMR spectroscopy. Upon complete conversion to **3**, no further HCOOH generation was observed. This suggests that **3** may be a catalytically dormant species and that **2** is the active species. This hypothesis was further investigated by studying the energetics of the hydride transfer to CO_2 for complexes **2** and **3** by DFT calculations (BP86, def2-TZVP), using R = phenyl on the sulfone group for computational simplicity (Fig. 4). Complex

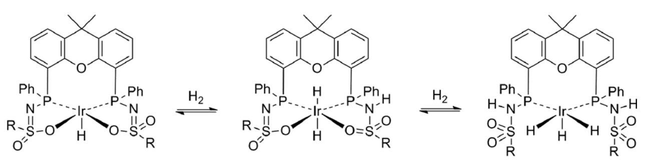

Scheme 1 Conversion to **3** from **1** upon addition of two equivalents of H_2.

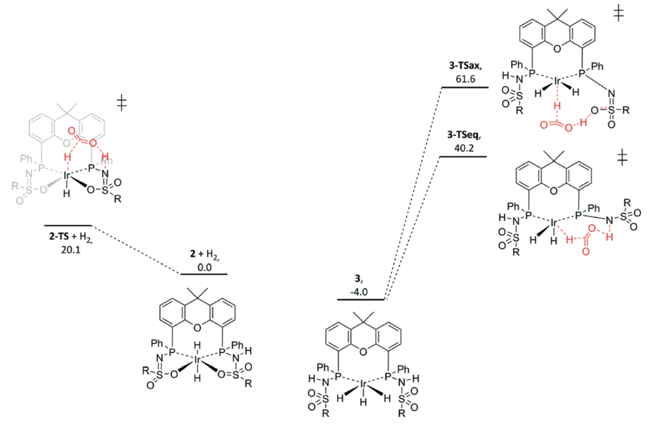

Fig. 4 DFT-calculated potential energy diagram of hydride transfer to CO_2 from complexes **2** and **3**. ΔG^0_{298K} in kcal mol^{-1}, R = phenyl (Turbomole,[17] BP86, def2-TZVP).

3 is lower in energy than **2** ($\Delta\Delta G^0_{298K}$ = −4 kcal mol^{-1}), which is in agreement with the observation of **3** by ^{1}H NMR spectroscopy. For species **2**, hydride transfer to CO_2 *via* transition state **2-TS** has a reasonable activation barrier of 20.1 kcal mol^{-1}, given the applied catalytic conditions. In complex **3**, hydride transfer to CO_2 could theoretically also occur. However, the transfer of either the axial hydride (**3TS-ax:** ΔG^0_{298K} = 65.6 kcal mol^{-1}) or one of the equatorial hydrides (**3TS-eq:** ΔG^0_{298K} = 44.2 kcal mol^{-1}) is considered too endergonic to be catalytically relevant (see the ESI† for details).

This observation is in line with the hypothesis that complex **3** is an off-cycle dormant species that is not directly involved in catalytic CO_2 hydrogenation (Scheme 2). Upon inspection of the computed structures of **2** and **3**, a correlation between the Ir–H bond length and the energy required for CO_2 insertion could be deduced (Fig. 5). The Ir–H bonds in species **2** (1.674 and 1.692 Å) are longer than those in **3** (Ir–H$_{eq}$, 1.631 and 1.632 Å; Ir–H$_{ax}$, 1.557 Å). The elongation in **2**, which results in weaker Ir–H bonds, likely originates from a mutual *trans* effect of the two hydride ligands. These bond length differences correlate nicely with the lower activation energy found for CO_2 insertion in **2** (20.1 kcal mol^{-1}) relative

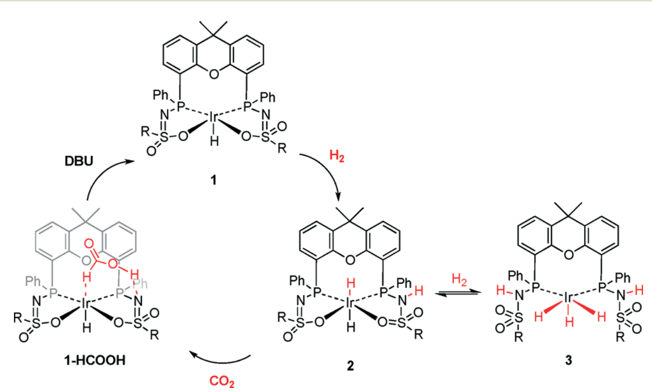

Scheme 2 Potential catalytic cycle of CO_2 hydrogenation from **1** with the active dihydride intermediate **2** and the dormant species **3** as the proposed off-cycle species.

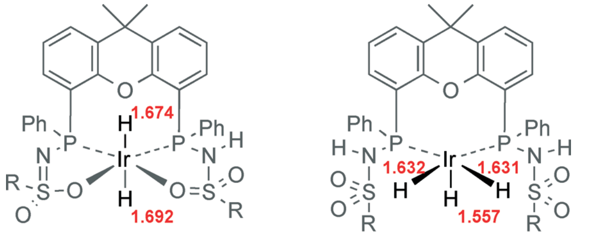

2 **3**

Fig. 5 Comparison of Ir–H bond lengths in the DFT-calculated optimized structures of complexes **2** and **3** (Turbomole,[18] BP86, def2-TZVP). The values are in Å, R = phenyl.

to **3** (44.2 and 65.6 kcal mol^{-1} for H_{eq} and H_{ax}, respectively). Our results are thus in agreement with the computational findings related to system **D**, demonstrating that *trans*-dihydride configurations allow for catalytically accessible energy barriers for CO_2 insertion.[11,12] Also, all transition states (**2-TS**, **3TS-ax** and **3TS-eq**) involve a stabilizing hydrogen bond interaction between the ligand backbone and CO_2. Improved catalyst design should focus on favoring the formation of **2** or analogues thereof. Research in this direction is currently ongoing in our laboratories.

Conclusions

Ir^{III}(H)(METAMORPhos) species **1** is able to catalytically hydrogenate CO_2 with a TOF of 18 h^{-1} in DMSO-d_6 at 373 K under 50 bar of CO_2/H_2 (1 : 1). A strong effect of the added base on the catalyst activity was observed: triethylamine led to a minor improvement, but DBU gave a significant enhancement of the reaction rate (TOF of 636 h^{-1}). The formation of a tight ion pair between formic acid and DBU ($HDBU^+ \cdot HCOO^-$) is suggested to provide the thermodynamic driving force. *In situ* NMR studies reveal that complex **1** is converted to a *fac*-trihydride complex (**3**) under CO_2/H_2 atmosphere (50 bar, 1 : 1) upon heating to 373 K. DFT calculations suggest that complex **3** is a dormant species in the catalytic cycle and *trans*-dihydride **2**, which is an intermediate in the conversion of **1** to **3**, is catalytically relevant. The formation of **3** is reversible, as complex **1** was regenerated upon release of pressure and heating to 373 K. Further studies to tune the reaction conditions for optimal catalytic activity and to design an optimized system should focus on the integration of a *trans*-dihydride arrangement.

Acknowledgements

This research was funded by a TOP grant from NWO-CW to J.N.H.R. We thank Prof. Dr. Bas de Bruin for helpful suggestions regarding the DFT calculations.

Notes and references

1 M. Aresta, A. Dibenedetto and A. Angelini, *Chem. Rev.*, 2014, **114**, 1709–1742; C. Maeda, Y. Miyazaki and T. Ema, *Catal. Sci. Technol.*, 2014, **4**, 1482–1497; A. M. Appel, J. E. Bercaw, A. B. Bocarsly, H. Dobbek, D. L. DuBois, M. Dupuis, J. G. Ferry, E. Fujita, R. Hille, P. J. A. Kenis, C. A. Kerfeld, R. H. Morris, C. H. F. Peden, A. R. Portis, S. W. Ragsdale, T. B. Rauchfuss, J. N. H. Reek, L. C. Seefeldt, R. K. Thauer and G. L. Waldrop, *Chem. Rev.*, 2013, **113**, 6621–6658; G. Centi, E. A. Quadrelli and S. Perathoner, *Energy Environ. Sci.*, 2013, **6**, 1711–1731; N. Kielland, C. J. Whiteoak and A. W. Kleij, *Adv. Synth. Catal.*, 2013, **355**, 2115–2138; C. Ziebart, C. Federsel, P. Anbarasan, R. Jackstell, W. Baumann, A. Spannenberg and M. Beller, *J. Am. Chem. Soc.*, 2012, **134**, 20701–20704; A. Boddien, D. Mellmann, F. Gärtner, R. Jackstell, H. Junge, P. J. Dyson, G. Laurenczy, R. Ludwig and M. Beller, *Science*, 2011, **333**, 1733–1736; M. Cokoja, C. Bruckmeier, B. Rieger, W. A. Herrmann and F. E. Kühn, *Angew. Chem., Int. Ed.*, 2011, **50**, 8510–8537; C. Federsel, A. Boddien, R. Jackstell, R. Jennerjahn, P. J. Dyson, R. Scopelliti, G. Laurenczy and M. Beller, *Angew. Chem., Int. Ed.*, 2010, **49**, 9777–9780; C. Federsel, R. Jackstell and M. Beller, *Angew. Chem., Int. Ed.*, 2010, **49**, 6254–6257.

2 For a selection of reviews, see: A. K. Singh, S. Singh and A. Kumar, *Catal. Sci. Technol.*, 2015, DOI: 10.1039/c5cy01276g; W.-H. Wang, Y. Himeda, J. T. Muckerman and E. Fujita, *Adv. Inorg. Chem.*, 2014, **66**, 189–222; M. Grasemann and G. Laurenczy, *Energy Environ. Sci.*, 2012, **5**, 8171–8181; T. Schaub and R. A. Paciello, *Angew. Chem., Int. Ed.*, 2011, **50**, 7278–7282; W. Reutemann and H. Kieczka, *Formic Acid, Ullmann's Encyclopedia of Industrial Chemistry*, Wiley-VCH, Weinheim, 6th edn, 2011.

3 R. Tanaka, M. Yamashita and K. Nozaki, *J. Am. Chem. Soc.*, 2009, **131**, 14168–14169; See also: I. Osadchuk, T. Tamm and M. S. G. Ahlquist, *Organometallics*, 2015, DOI: 10.1021/acs.organomet.5b00448.

4 J. F. Hull, Y. Himeda, W.-H. Wang, B. Hashiguchi, R. Periana, D. J. Szalda, J. T. Muckerman and E. Fujita, *Nat. Chem.*, 2012, **4**, 383–388.

5 G. A. Filonenko, M. P. Conley, C. Copéret, M. Lutz, E. J. M. Hensen and E. A. Pidko, *ACS Catal.*, 2013, **3**, 2522–2526; G. A. Filonenko, R. van Putten, E. N. Schulpen, E. J. M. Hensen and E. A. Pidko, *ChemCatChem*, 2014, **6**, 1526–1530; See also: G. A. Filonenko, D. Smykowski, B. M. Szyja, G. Li, J. Szczygie, E. J. M. Hensen and E. A. Pidko, *ACS Catal.*, 2015, **5**, 1145–1154.

6 X. Yang, *ACS Catal.*, 2011, **1**, 849–854; M. S. G. Ahlquist, *J. Mol. Catal. A: Chem.*, 2010, **324**, 3–8; R. Tanaka, M. Yamashita, L. W. Chung, K. Morokuma and K. Nozaki, *Organometallics*, 2011, **30**, 6742–6750.

7 W. Wang, J. T. Muckerman, E. Fujita and Y. Himeda, *ACS Catal.*, 2013, **3**, 856–860; W. Wang, J. F. Hull, J. T. Muckerman, E. Fujita and Y. Himeda, *Energy Environ. Sci.*, 2012, **5**, 7923–7926.

8 G. A. Filonenko, E. J. M. Hensen and E. A. Pidko, *ACS Catal.*, 2014, **4**, 2667–2671; G. A. Filonenko, E. J. M. Hensen and E. A. Pidko, *Catal. Sci. Technol.*, 2014, **4**, 3474–3485.

9 E. A. Bielinski, P. O. Lagaditis, Y. Zhang, B. Q. Mercado, C. Würtele, W. H. Bernskoetter, N. Hazari and S. Schneider, *J. Am. Chem. Soc.*, 2014, **136**, 10234–10237.

10 C. Yin, Z. Xu, S.-Y. Yang, S. M. Ng, K. Y. Wong, Z. Lin and C. P. Lau, *Organometallics*, 2001, **20**, 1216–1222; C. A. Huff, J. W. Kampf and M. S. Sanford, *Organometallics*, 2012, **31**, 4643–4645; P. Kang, C. Cheng, Z. Chen, C. K. Schauer, T. J. Meyer and M. Brookhart, *J. Am. Chem. Soc.*, 2012, **134**, 5500–5503; C. A. Huff and M. S. Sanford, *ACS Catal.*, 2013, **3**, 2412–2416; P. Kang, T. J. Meyer and M. Brookhart, *Chem. Sci.*, 2013, **4**, 3497–3502; L. Cao, C. Sun, N. Sun, L. Meng and D. Chen, *Dalton Trans.*, 2013, **42**, 5755–5763; T. W. Myers and L. A. Berben, *Chem. Sci.*, 2014, **5**, 2771–2777; L. S. Jongbloed, B. de Bruin, J. N. H. Reek, M. Lutz and J. I. van der Vlugt, *Chem. – Eur. J.*, 2015, **21**, 7297–7305; L. S. Jongbloed, B. de Bruin, J. N. H. Reek, M. Lutz and J. I. van der Vlugt, *Catal. Sci. Technol.*, under revision.

11 T. J. Schmeier, G. E. Dobereiner, R. H. Crabtree and N. Hazari, *J. Am. Chem. Soc.*, 2011, **133**, 9274–9277.

12 B. Mondal, F. Neese and S. Ye, *Inorg. Chem.*, 2015, **54**, 7192–7198; J. T. Muckerman, P. Achord, C. Creutz, D. E. Polyansky and E. Fujita, *Proc. Natl. Acad. Sci. U. S. A.*, 2012, **109**, 15657–15662.

13 S. Oldenhof, B. de Bruin, M. Lutz, M. A. Siegler, F. W. Patureau, J. I. van der Vlugt and J. N. H. Reek, *Chem. – Eur. J.*, 2013, **19**, 11507–11511; S. Oldenhof, M. Lutz, B. de Bruin, J. I. van der Vlugt and J. N. H. Reek, *Chem. Sci.*, 2015, **6**, 1027–1034.

14 Related CO_2 hydrogenation under acidic conditions: H. Hayashi, S. Ogo and S. Fukuzumi, *Chem. Commun.*, 2004, 2714–2715; S. Ogo, R. Kabe, H. Hayashi, R. Harada and S. Fukuzumi, *Dalton Trans.*, 2006, 4657–4663; S. Moret, P. J. Dyson and G. Laurenczy, *Nat. Commun.*, 2014, **5**, 4017.

15 D. J. Fox, S. B. Duckett, C. Flaschenriem, W. W. Brennessel, J. Schneider, A. Gunay and R. Eisenberg, *Inorg. Chem.*, 2006, **45**, 7197–7209; B. A. J. Pontiggia, A. B. Chaplin and A. S. Weller, *J. Organomet. Chem.*, 2011, **696**, 2870–2876; M. A. Esteruelas, M. Oliván and A. Vélez, *Inorg. Chem.*, 2013, **52**, 5339–5349.

16 S. Oldenhof, B. de Bruin, M. Lutz, M. A. Siegler, F. W. Patureau, J. I. van der Vlugt and J. N. H. Reek, *Organometallics*, 2014, **33**, 7293–7298; S. Oldenhof, F. G. Terrade, M. Lutz, J. I. van der Vlugt and J. N. H. Reek, *Organometallics*, 2015, **34**, 3209–3215; S. Oldenhof, J. I. van der Vlugt and J. N. H. Reek, *Chem. Commun.*, 2015, **51**, 15200–15203; See also: F. F. W. Patureau, S. de Boer, M. Kuil, J. Meeuwissen, P.-A. R. Breuil, M. A. Siegler, A. L. Spek, A. J. Sandee, B. de Bruin and J. N. H. Reek, *J. Am. Chem. Soc.*, 2009, **131**, 6683–6685; F. G. Terrade, M. Lutz, J. I. van der Vlugt and J. N. H. Reek, *Eur. J. Inorg. Chem.*, 2014, 1826–1835.

17 R. Ahlrichs, *Turbomole Version 5*, University of Karlsruhe, Germany, 2002; *PQS version 2.4, Parallel Quantum Solutions*, Fayettevile, AR (USA), 2001; The baker optimizer is available separately from PQS upon request: I. Baker, *J. Comput. Chem.*, 1986, **7**, 385–395; P. H. M. Budzelaar, *J. Comput. Chem.*, 2007, **28**, 2226–2236; A. D. Becke, *Phys. Rev. A: At., Mol., Opt. Phys.*, 1988, **38**, 3098–3100; J. P. Perdew, *Phys. Rev. B: Condens. Matter Mater. Phys.*, 1986, **33**, 8822–8824.

18 A. Bartoszewicz, N. Ahlsten and B. Martín-Matute, *Chem. – Eur. J.*, 2013, **19**, 7274–7302; R. Crabtree, *Acc. Chem. Res.*, 1979, **12**, 331–337; S. P. Smidt, A. Pfaltz, E. Martínez-Viviente, P. S. Pregosin and A. Albinati, *Organometallics*, 2003, **22**, 1000–1009.